

Tora: Trajectory-oriented Diffusion Transformer for Video Generation

Zhenghao Zhang^{1*}, Junchao Liao^{1*}, Menghao Li¹, Long Qin¹, Weizhi Wang¹

¹Alibaba Group

{zhangzhenghao.zzh, liaojunchao.ljc, limenghao.lmh, ql362507, wangweizhi.wwz}@alibaba-inc.com
projectpage: https://ali-videoai.github.io/tora_video/



Figure 1: Tora is capable of generating videos guided by trajectories, images, texts, or combinations thereof. Leveraging the scalability of DiT, the generated movement not only adheres precisely to the trajectory but also effectively emulates physical world dynamics. Notably, when generating videos at a 720p resolution, Tora maintains stable motion control for up to 204 frames. Due to limited space, we summarize the captions. Highly recommend viewing the video results on the project page.

Abstract

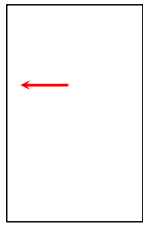
Recent advancements in Diffusion Transformer (DiT) have demonstrated remarkable proficiency in producing high-quality video content. Nonetheless, the potential of transformer-based diffusion models for effectively generating videos with controllable motion remains an area of limited exploration. This paper introduces Tora, the first trajectory-oriented DiT framework that integrates textual, visual, and trajectory conditions concurrently for video generation. Specifically, Tora consists of a Trajectory Extractor (TE), a Spatial-Temporal DiT, and a Motion-guidance Fuser (MGF). The TE encodes arbitrary trajectories into hierarchical spacetime motion patches with a 3D video compression network. The MGF integrates the motion patches into the DiT blocks to generate consistent videos following trajectories. Our design aligns seamlessly with DiT’s scalability, allowing precise control of video content’s dynamics with diverse durations, aspect ratios, and resolutions. Extensive experiments demonstrate Tora’s excellence in achieving high motion fidelity, while also meticulously simulating the movement of the physical world.

*These authors contributed equally.

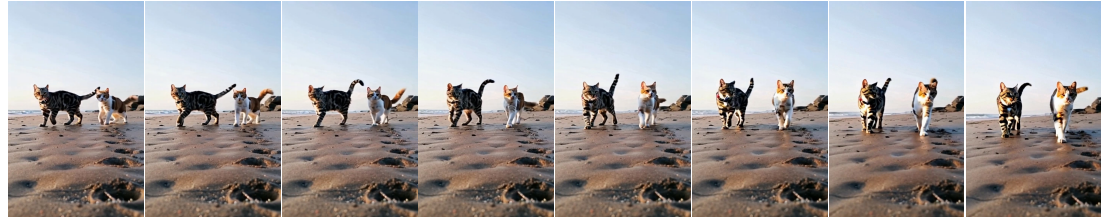
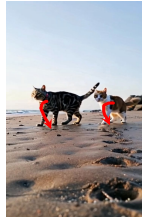
Introduction

Diffusion models (Dhariwal and Nichol 2021; Ramesh et al. 2022) have demonstrated their capability to generate diverse and high-quality images or videos. Previously, video diffusion models (Ho et al. 2022b; Blattmann et al. 2023; Zhang et al. 2023a) predominantly employed U-Net architectures (Olaf Ronneberger 2015), focusing primarily on synthesizing videos of limited duration, typically around two seconds, and were constrained to fixed resolutions and aspect ratios. Recently, Sora (Brooks et al. 2024), a text-to-video generation model leveraging Diffusion Transformer (DiT) (Peebles and Xie 2023), has showcased video generation capabilities that significantly outstrip current state-of-the-art methods. Sora excels not only in the production of high-quality videos ranging from 10 to 60 seconds, but also distinguishes itself through its capacity to handle diverse resolutions, various aspect ratios, adherence to the laws of actual physics.

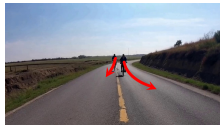
Video generation entails the creation of consistent motion within a sequence of generated images, thereby emphasizing the importance of motion control. Prior research endeavor-



A joyful brown puppy turns its head happily while playing on a green grassy field.



On a bright, sunny day, two adorable kittens walk side by side along the golden sands of a serene beach.



Two men cycled on the highway under a clear, sunny sky.



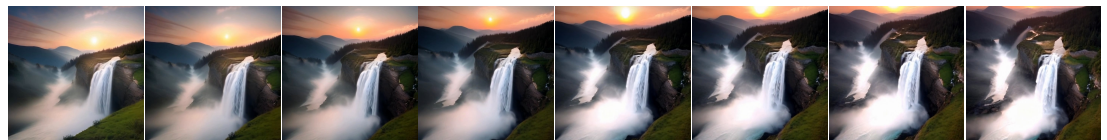
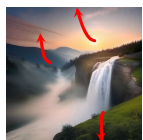
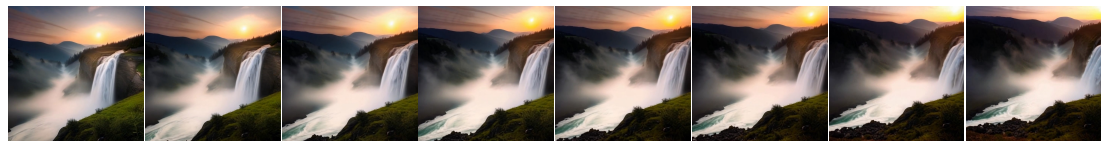
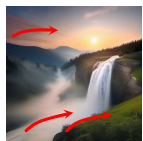
A crucian carp swims gracefully across the red, rocky surface of Mars.



A flock of seagulls soars gracefully through the vibrant underwater world filled with colorful coral reefs.



A sleek sports car races along a mountain road as snowflakes gradually fall, slowly covering the entire path.



A dynamic aerial shot showcasing a mountain waterfall cascades down in the early morning light.

Figure 2: More generated samples. Tora accommodates a wide array of visual conditions, encompassing both single starting frames and combinations of initial and final frames (as seen in the sixth row), and expertly handles multiple trajectories to precisely manipulate multiple objects. It adeptly facilitates video generation across diverse aspect ratios, resolutions, and durations, thereby ensuring flexible and adaptive content creation. Check out our project page for all video demos.

ors, such as VideoComposer (Wang et al. 2023a) and Drag-NUWA (Yin et al. 2023), have successfully implemented

generalized motion manipulation techniques. These methods typically involve extracting motion vectors and optical

flow data to direct the video generation models. Building upon these advancements, MotionCtrl (Wang et al. 2023b) innovates by separately managing camera movements and object motions, thereby expanding the achievable motion ranges and patterns. Despite promising controllable motion quality, these methods are limited to generating videos of up to 16 frames in length and at a lower, fixed resolution. Moreover, limitations in the number of frames can hinder the seamless portrayal of motion, particularly in scenarios involving significant positional shifts. This often leads to issues such as motion blur, appearance distortions, and unnatural movements, such as parallel drifting, which deviate from real-world physical dynamics.

To address these challenges, we introduce Tora—a pioneering DiT model that simultaneously integrates text, image, and trajectory data, ensuring meticulous and versatile control over video content. Tora innovatively embeds the provided trajectory into multiple patches, enhancing motion fluidity and more closely adhering to the natural principles of object kinetics, leveraging its remarkable scaling properties. Notably, our work adopts OpenSora (Zheng et al. 2024), an open-source version of Sora, as the foundational DiT framework. To facilitate motion control, we design two innovative modules: the Trajectory Extractor (TE), which transforms arbitrary trajectories into hierarchical spacetime motion patches, and the Motion-guidance Fuser (MGF), meticulously crafted to integrate these motion patches within the stacked architecture of DiT blocks. More specifically, TE initially converts positional displacements along trajectories between successive frames into the RGB domain via flow visualization techniques. These visualized displacements undergo Gaussian filtering to mitigate scattered issues. Subsequently, a 3D Variational Autoencoder (VAE) (Kingma and Welling 2013) encodes trajectory visualizations into spacetime motion latents, which share the same latent space with video patches. The motion latents are then decomposed into multiple levels of motion conditions via a series of stacked lightweight modules. Our VAE architecture is inspired by MAGVIT-v2 (Yu et al. 2023b) but simplified by foregoing codebook dependencies and utilizing solely VAE reconstruction loss for training. The MGF integrates adaptive normalization layers (Perez et al. 2018) to infuse multi-level motion conditions into the corresponding DiT blocks. We explored various adaptations of transformer blocks including adaptive layer normalization, cross-attention, and extra channel connections to inject the motion conditions. Among these, adaptive layer normalization emerged as the most effective to generate consistent videos following trajectories.

To train Tora, annotated videos with captions and movement trajectories are essential. We adapt OpenSora’s workflow to transform raw videos into high-quality video-text pairs and leverage an optical flow estimator (Xu et al. 2023) for trajectory extraction. Significantly, we combine motion segmentation results (Zhao et al. 2022) with flow scores to filter out instances that primarily contain camera movement. This strategic approach improves our ability to accurately follow the trajectory of specific objects within videos. As a result, this careful selection process leads to the creation of a dataset containing 630k high-quality video clips with

consistent motion. With an adapter-like strategy (Mou et al. 2024), we solely train the temporal blocks, together with the TE and MGF. This strategy seamlessly integrates DiT’s inherent generative knowledge with external motion signals.

The main contributions of our work are as follows:

- We introduce Tora, the first trajectory-oriented DiT for video generation. As illustrated in Figure 2, Tora seamlessly integrates a broad range of visual and trajectory instructions, thereby proficiently enabling the creation of motion-manipulable videos.
- To align with the scalability of DiT, we design a novel trajectory extractor and a motion-guidance fusion mechanism to obtain spacetime motion patches, subsequently injecting these patches into DiT blocks. We ablate several architecture choices and offer empirical baselines for future research in DiT-based motion control.
- Experiments demonstrate that Tora is capable of generating 720p resolution videos with varying aspect ratios, extending up to 204 frames, all guided by the specified trajectories. Furthermore, it demonstrates superiority in simulating movements within the physical world.

Related Work

Diffusion models for Video Generation

Diffusion models have demonstrated an impressive capability to generate high-quality video samples. Previous research (Ho et al. 2022b,a; Singer et al. 2022; Wu et al. 2023; Khachatryan et al. 2023; Zhang et al. 2023b) commonly used video diffusion models (VDMs) that incorporated temporal convolutional and attention layers into the pre-trained image diffusion models. Subsequently, VideoCrafter (Chen et al. 2023) and SVD (Blattmann et al. 2023) expand the application of video diffusion models to larger datasets, while TF-T2V (Wang et al. 2024a) directly learn from extensive text-free videos. Lumiere (Bar-Tal et al. 2024) introduces the concept of temporal downsampling within the 3D UNet framework. Nonetheless, these methods encounter limitations in generating long videos, owing to the inherent constraints on capacity and scalability within the UNet design. Conversely, DiT-based models (Brooks et al. 2024; Zheng et al. 2024; Bao et al. 2024) can directly generate videos extending up to tens of seconds. Sora (Brooks et al. 2024) converts visual data into a unified representation, facilitating large-scale training and enabling the generation of 1-minute high-definition video. Vidu (Bao et al. 2024) is capable of generating both realistic and imaginative videos in various aspect ratios and resolutions. For our study, we adopt OpenSora (Zheng et al. 2024) as the foundational model, which is an open-source alternative to Sora.

Motion control in Video Generation

To better control motion in generated video, a multitude of studies have endeavored to introduce diverse motion signals in VDMs. Pioneering works like MotionDirector (Zhao et al. 2023) and VMC (Jeong, Park, and Ye 2024) have utilized reference videos to extract motion patterns applicable to diverse video generations. VideoComposer (Wang et al.

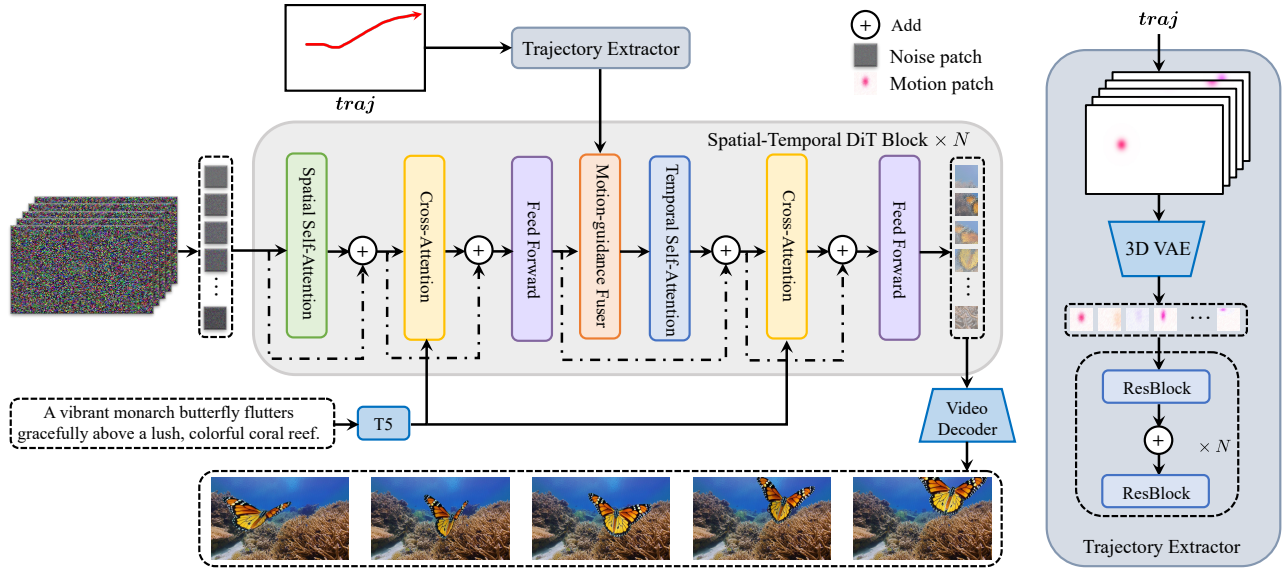


Figure 3: Overview of the Tora Architecture. For achieving trajectory-controlled DiT-based video generation, we introduce two novel modules: the Trajectory Extractor and the Motion-guidance Fuser. The Trajectory Extractor employs a 3D motion VAE to embed trajectory vectors into the same latent space as video patches, effectively preserving motion information across consecutive frames. Subsequently, it uses stacked convolutional layers to extract hierarchical motion features. The Motion-guidance Fuser utilizes adaptive normalization layers to seamlessly inject these multi-level motion conditions into the corresponding DiT blocks, ensuring the generation of videos that consistently follow the defined trajectories. Our method aligns with the scalability of DiT, enabling the creation of high-resolution, motion-controllable videos with prolonged durations.

2023a) expands upon this by adopting depth maps, sketches, or motion vectors from references as conditional inputs for motion control. Nonetheless, these methodologies are limited to reproducing existing motion patterns. Conversely, approaches that leverage trajectories or bounding boxes (Yin et al. 2023; Dai et al. 2023; Wang et al. 2024b) in video generation promise greater adaptability and user accessibility. DragNUWA (Yin et al. 2023) breaks new ground by integrating trajectory-based conditioning into VDMs, facilitating complex camera and object movements. AnimateAnything (Dai et al. 2023) employs motion masks for precise control over the moving regions. TrailBlazer (Wan-Duo Kurt Ma 2023), employs explicit attention mechanisms to maneuver generated objects along precise trajectories. MotionCtrl (Wang et al. 2024b) facilitates more flexible control, allowing separate adjustment of both camera movements and individual object motions. However, all of them often yield noticeable artifacts in both motion consistency and visual presentation when applied to longer video sequences. In contrast, our method first integrates trajectories into DiT architecture, specifically designed to accommodate scaling properties. This enables motion fluidity and closer adherence to the physical world.

Methodology

Preliminary

Latent Video Diffusion Model (LVDM). The LVDM enhances the stable diffusion model (Ramesh et al. 2022) by integrating a 3D U-Net, thereby empowering efficient video

data processing. This 3D U-Net design augments each spatial convolution with an additional temporal convolution and follows each spatial attention block with a corresponding temporal attention block. It is optimized employing a noise-prediction objective function:

$$l_{\epsilon} = \|\epsilon - \epsilon_{\theta}(z_t, t, c)\|_2^2, \quad (1)$$

Here, $\epsilon_{\theta}(\cdot)$ signifies the 3D U-Net’s noise prediction function. The condition c is guided into the U-Net using cross-attention for adjustment. Meanwhile, z_t denotes the noisy hidden state, evolving like a Markov chain that progressively adds Gaussian noise to the initial latent state z_0 :

$$z_t = \sqrt{\bar{\alpha}_t}z_0 + \sqrt{1 - \bar{\alpha}_t}\epsilon, \quad \epsilon \sim \mathcal{N}(0, I), \quad (2)$$

where $\bar{\alpha}_t = \prod_{i=1}^t (1 - \beta_i)$ and β_t is a coefficient that controls the noise strength in step t .

Diffusion Transformer (DiT). The DiT (Peebles and Xie 2023) constitutes a seminal architectural innovation that synergistically combines the advantages of diffusion models with the transformer architectures (Vaswani et al. 2017). This integration is purposed to transcend the limitations of traditional U-Net-based LDMs, augmenting their performance, versatility, and scalability. While maintaining the overarching formulation congruent with established LDM frameworks, the paradigm shift resides in the substitution of the U-Net with a transformer architecture for the denoising function $\epsilon_{\theta}(\cdot)$ learning, thereby marking a pivotal advance in the realm of generative modeling.

Tora

Tora adopts OpenSora as the foundational model for its DiT architecture. To facilitate precise and user-friendly motion control across diverse durations, Tora introduces two novel motion-processing components: the Trajectory Extractor (TE) and the Motion-guidance Fuser (MGF). These modules serve to encode provided trajectories into multi-level spacetime motion patches, meticulously integrating these patches within the stacked structure of DiT blocks. An overview of Tora’s workflow is depicted in Figure 3.

Spatial-Temporal DiT. The ST-DiT architecture incorporates two distinct block types: the Spatial DiT Block (S-DiT-B) and the Temporal DiT Block (T-DiT-B), arranged in an alternating sequence. The S-DiT-B comprises two attention layers, each performing Spatial Self-Attention (SSA) and Cross-Attention sequentially, succeeded by a point-wise feed-forward layer that serves to connect adjacent T-DiT-B block. Notably, the T-DiT-B modifies this schema solely by substituting SSA with Temporal Self-Attention (TSA), preserving architectural coherence. Within each block, the input, upon undergoing normalization, is concatenated back to the block’s output via skip-connections. By leveraging the ability to process variable-length sequences, the denoising ST-DiT can handle videos of variable durations.

During processing, a video autoencoder (Yu et al. 2023a) is first employed to diminish both spatial and temporal dimensions of videos. To elaborate, it encodes the input video $X \in \mathbb{R}^{L \times H \times W \times 3}$ into video latent $z_0 \in \mathbb{R}^{l \times h \times w \times 4}$, where L denotes the video length and $l = L/4$, $h = H/8$, $w = W/8$. z_0 is next “patchified”, resulting in a sequence of input tokens $I \in \mathbb{R}^{l \times s \times d}$. Here, $s = hw/p^2$ and p denotes the patch size. I is then forwarded to the ST-DiT, which models these compressed representations. In both SSA and TSA, standard Attention is performed using Query (Q), Key (K), and Value (V) matrices:

$$Q = W_Q \cdot I_{norm}; K = W_K \cdot I_{norm}; V = W_V \cdot I_{norm} \quad (3)$$

Here, I_{norm} represents the normalized I , W_Q, W_K, W_V are learnable projection matrices. The textual prompt is first embedded utilizing a T5 text encoder. The cross-attention mechanism is employed between the embedded prompt and the intermediate features from either the SSA or the TSA.

Trajectory Extractor. Trajectories have proven to be a more user-friendly method for controlling the motion of generated videos. Specifically, given a trajectory $traj = \{(x_i, y_i)\}_{i=0}^{L-1}$, where (x_i, y_i) denotes the spatial position (x, y) at the i -th frame the trajectory passes through. Previous studies primarily encode the horizontal offset $u(x_i, y_i)$ and the vertical offset $v(x_i, y_i)$ as the motion condition for (x_i, y_i) :

$$u(x_i, y_i) = x_{i+1} - x_i; v(x_i, y_i) = y_{i+1} - y_i. \quad (4)$$

However, the DiT model employs a video autoencoder and a patchification process to convert the video into video patches. Here, each patch is derived across multiple frames, rendering it inappropriate to straightforwardly employ frame-to-frame offsets. To address this, our TE converts the trajectory into motion patches, which inhabit the

same latent space as the video patches. Particularly, we begin by transforming the $traj$ into a trajectory map $g \in \mathbb{R}^{L \times H \times W \times 2}$, enhanced with a Gaussian Filter to mitigate scatter. Notably, the first frame employs a fully-zero map. Afterward, the trajectory map g is translated into the RGB color space, producing $g_{vis} \in \mathbb{R}^{L \times H \times W \times 3}$ through a flow visualization technique. We use a 3D VAE to compress trajectory maps, achieving an 8x spatial and 4x temporal reduction, aligning with OpenSora framework. Our 3D VAE is based on the Magvit-v2 architecture, with spatial compression initialized using the VAE of SDXL (Podell et al. 2023) to accelerate convergence. We train the model using only reconstruction loss to obtain the compact motion latent representation $g_m \in \mathbb{R}^{l \times h \times w \times 4}$ from the g_{vis} .

To match the size of the video patches, we use the same patch size on g_m and encode it using a series of convolutional layers, resulting in spacetime motion patches $f \in \mathbb{R}^{l \times s \times d_v}$. Here d_v is the dimension of motion patches. The output of each convolutional layer is skip-connected to the input of the next layer to extract multi-level motion features:

$$f_i = Conv^i(f_{i-1}) + f_{i-1}. \quad (5)$$

where f_i is the motion condition for i -th ST-DiT block.

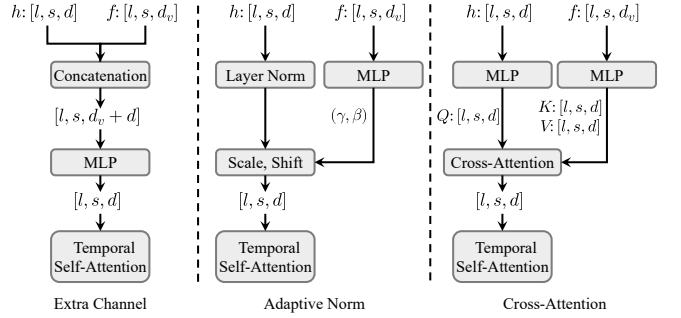


Figure 4: Different designs of the Motion-guidance Fuser for incorporating trajectory conditioning. Adaptive Norm demonstrates the best performance.

Motion-guidance Fuser. To incorporate DiT-based video generation with the trajectory, we explore three variants of fusion architectures that inject motion patches into each ST-DiT block. These designs are illustrated in Figure 4.

- Extra channel connections. Denote $h_i \in \mathbb{R}^{l \times s \times d}$ as the resultant output from the i -th block of the ST-DiT. Following the widespread use of concatenation in GAN-based LVDM, the motion patches are simply concatenated with the previous hidden state h_{i-1} along the channel dimension. An additional convolution layer is then added to maintain the same latent size:

$$h_i = Conv([h_{i-1}, f_i]) + h_{i-1}. \quad (6)$$

- Adaptive Norm layer. Inspired by the adaptive normalization layers employed in GANs, we initially convert f_i into scale γ_i and shift β_i by adding two zero-initialized convolution layers into the ST-DiT block. Subsequently, γ_i and β_i are integrated into h_i through a straightforward linear projection:

$$h_i = \gamma_i \cdot h_{i-1} + \beta_i + h_{i-1}. \quad (7)$$

- Cross-Attention layer. The ST-DiT block has been modified to include an additional Cross-Attention layer following the SSA or TSA, with the motion patches serving as the key and value to integrate with the hidden state h :

$$h_i = \text{CrossAttn}([h_{i-1}, f_i]) + h_{i-1}. \quad (8)$$

We experiment with three types of fusion architectures, finding that the adaptive norm demonstrates the best generation performance and compute efficiency. For the remainder of the paper, MGF employs the adaptive norm layer unless otherwise specified.

Training Strategy and Data Processing

To achieve fine-grained control while generating a video using arbitrary trajectories, as well as text, images, or their composites, we introduce several training strategies for different condition injections.

Motion condition training. Inspired by DragNUWA and MotionCtrl, we use a two-stage training approach for trajectory learning. In the first stage, we extract the dense optical flow (Xu et al. 2023) from the training video as the trajectory, offering richer information to accelerate motion learning. During the second stage, to adapt the model from complete optical flow to more user-friendly trajectories, we select a random sample of 1 to N object trajectories from the optical flow according to the motion segmentation results and flow scores. To address the scattered issues of sparse trajectories, we apply a Gaussian filter for refinement. Upon completion of the two-stage training phase, Tora enables flexible motion control using arbitrary trajectories.

Image condition training. We follow the mask strategy employed by OpenSora to support visual conditioning. Specifically, we randomly unmask frames during training, and the video patches of the unmasked frames are not subjected to any noise. This enables our Tora model to seamlessly integrate text, images, and trajectories into a unified model.

Data Processing. For Tora, it is crucial that the video clips in the training dataset are annotated with both captions and movement trajectories (optical flow). To fulfill this requirement, we employ a structured data processing method. Initially, raw videos are segmented into shorter clips based on scene detection. Subsequently, these clips are evaluated using aesthetic scores. Given our criteria, static videos are excluded by retaining only those with optical flow scores exceeding 3. To better obtain object trajectories, we employ the results of motion segmentation and camera detection to remove instances that primarily contain camera trajectories in dynamic scenes. Additionally, dramatic camera or object motions in some videos can cause significant optical flow deviations, interfering with trajectory training. Consequently, we retain these videos with a probability of $(1 - \text{score}/100)$. For eligible videos, we generate captions using the PLLaVA model (Xu et al. 2024). To balance speed and performance, we utilize the 13B version.

Experiments

Experimental Setup

Implementation Details. We train Tora based on OpenSora v1.2 weights. The resolutions of the training videos vary

from 144p to 720p. The numbers of frames range from 51 to 204. To balance the training FLOP and required memory for different resolutions and numbers of frames per iteration, we adjust the batch size accordingly from 1 to 25. We use Adam Optimizer (Kingma and Ba 2015) with a learning rate of 2×10^{-5} on 4 NVIDIA A100. We train Tora with the dense optical flow for 2 epochs and fine-tune it with the sparse optical flow for 1 epoch. The maximum number of sampling trajectories N is set to 16. The inference step and the guidance scale are set to 30 and 7.0, respectively.

Dataset. Our training videos are sourced from three datasets: 1) Panda-70M (Chen et al. 2024), from which we use the training-10M subset containing high-quality videos; 2) Mixkit (Envato 2024); and 3) Interval Video. After applying our data processing pipeline, we select approximately 630k eligible videos for the training dataset. For inference, we curate 185 clips with diverse motion trajectories and scenes, to serve as a new benchmark for evaluating the motion controllability. Additional information about the construction of the evaluation datasets is available in our supplementary materials.

Metrics. We leverage standard metrics such as Fréchet Video Distance (FVD) (Unterthiner et al. 2018), and CLIP Similarity (CLIPSIM) (Wu et al. 2021) to quantitatively evaluate video quality. For assessing motion controllability, we leverage Trajectory Error (TrajError), which computes the average distance between the generated and pre-defined trajectories. Human evaluation is also introduced.

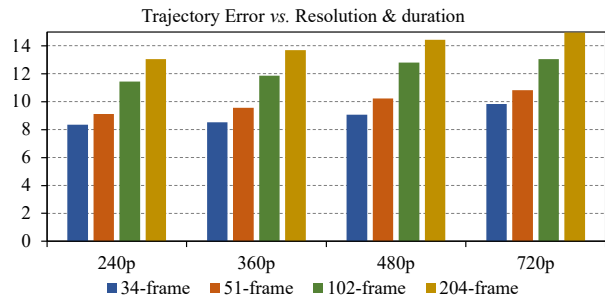


Figure 5: Comparison of Trajectory Error across various resolutions and durations. Unlike U-Net models, our method maintains motion control with a gradual increase in error.

Quantitative and Qualitative Results

We compare our method against prevalent motion-guided video generation approaches. The evaluation is conducted under three settings: 16, 64, and 128 frames, all with a resolution of 512×512 for fair comparison. The provided trajectories are clipped to accommodate different evaluated video lengths. For most U-Net based methods, we employ sequenced inference, wherein the last frame generated by the previous batch serves as the visual condition for the current batch, aligning with their inference settings. As illustrated in Table 1, under the 16-frame setting commonly employed by U-Net based methods, MotionCtrl and DragNUWA exhibit better alignment with the provided trajectories but are still

Method	FVD (\downarrow)			CLIPSIM (\uparrow)			TrajError (\downarrow)		
	16-frame	64-frame	128-frame	16-frame	64-frame	128-frame	16-frame	64-frame	128-frame
VideoComposer (Wang et al. 2023a)	529	668	856	0.2335	0.2284	0.2236	15.11	29.14	58.76
DragNUWA (Yin et al. 2023)	475	593	784	0.2385	0.2341	0.2305	10.04	17.33	41.25
AnimateAnything (Dai et al. 2023)	487	602	775	0.2399	0.2342	0.2313	13.39	27.28	51.33
TrailBlazer (Wan-Duo Kurt Ma 2023)	459	581	756	0.2403	0.2351	0.2322	11.68	19.47	44.10
MotionCtrl (Wang et al. 2024b)	463	572	731	0.2412	0.2376	0.2331	9.42	16.46	38.39
Ours	438	460	494	0.2447	0.2435	0.2418	7.23	8.45	11.72

Table 1: Quantitative comparisons with state-of-the-art motion-controllable video generation models. As the number of generated frames increases, Tora demonstrates a growing performance advantage over the UNet-based methods, maintaining a high degree of stability in trajectory control.

weaker compared to our proposed Tora. As the frame count increases, the U-Net based methods show significant deviations in certain frames, with misalignment errors propagating and leading to deformation, motion blur, or object disappearance in subsequent sequences. In contrast, Tora demonstrates high robustness to varying frame numbers due to the integration of the transformer’s scaling ability. The movement generated by Tora is smoother and more aligned with the physical world. When evaluated under the 128-frame test setting, Tora’s trajectory accuracy surpasses other methods by a factor of 3 to 5, demonstrating its exceptional motion control capabilities. In Figure 5, we provide an analysis of the Trajectory Error across varying resolutions and durations. Unlike U-Net based models, which exhibit significant trajectory errors over time, Tora shows only a gradual increase in Trajectory Error as duration increases. This gradual increase in error aligns with the decrease in video quality observed in the DiT model as the duration extends. The results clearly indicate that our method maintains effective trajectory control over longer durations.

Method	FVD	CLIPSIM	TrajError
Sampling Frame	581	0.2304	27.61
Average Pooling	558	0.2325	20.97
3D VAE	513	0.2358	14.25

Table 2: Evaluations of the impact of different trajectory compression methods. The 3D VAE yields superior results in motion-conditioned encoding.

Figure 6 presents a comparative analysis of our proposed method against mainstream motion control techniques. In the first scenario, which involves the co-movement of two men, all methods are able to generate relatively accurate motion trajectories. However, our approach demonstrates superior visual quality. This advantage is primarily due to the utilization of longer sequence frames, which facilitate smoother motion trajectories and more realistic background rendering. For instance, in our generated bicycle scenario, the human legs exhibit realistic pedaling motions, whereas the output from DragNUWA features legs that appear almost horizontally floating, violating physical realism. Additionally, both DragNUWA and MotionCtrl suffer from significant motion blur towards the end of their videos. Furthermore, MotionCtrl introduces unintended camera movements

during the riding sequence, despite the absence of camera movement conditions. In another case, DragNUWA shows severe deformation of the lantern as the provided trajectory rises and falls continuously. Although MotionCtrl’s trajectory is relatively accurate, the resulting video fails to match the expected depiction of two lanterns. Overall, our method not only adheres closely to the provided trajectories but also minimizes object deformation, thereby ensuring higher fidelity in motion representation.

Ablation study

In this section, we conduct several ablation studies to analyze the effects of our design choices. All models are evaluated using 480p resolution, a 16:9 aspect ratio, and 204 frames.

Method	FVD	CLIPSIM	TrajError
Extra Channel	542	0.2329	21.07
Cross Attention	526	0.2354	18.36
Adaptive Norm	513	0.2358	14.25

Table 3: Different variants of motion fusion blocks employed in MGF. Adaptive Norm works best.

Trajectory Compression. To incorporate the trajectory vector within the same latent space as video patches, we investigate three distinct methods for trajectory compression, as summarized in Table 2. The first method samples the mid-frame as the keyframe for successive 4-frame intervals and employs patch-unshuffle for spatial compression. Despite its simplicity, this method proves suboptimal for motion control, primarily due to the potential flow estimation errors when encountering rapid motions or occlusions. Additionally, the magnified dissimilarity between patches induced by the chosen frame interval exacerbates learning challenges. The second method utilizes average pooling to gather successive frames. While this captures a general sense of movement, it inadvertently sacrifices precision by homogenizing the trajectory’s direction and magnitude, thereby diluting critical motion details. To preserve the trajectory information between consecutive frames as much as possible, we further employ a 3D VAE to extract the global context of successive trajectory intervals. The trajectory data is visually translated into an RGB image format to leverage existing 3D VAE weights. Extensive training on a large scale of

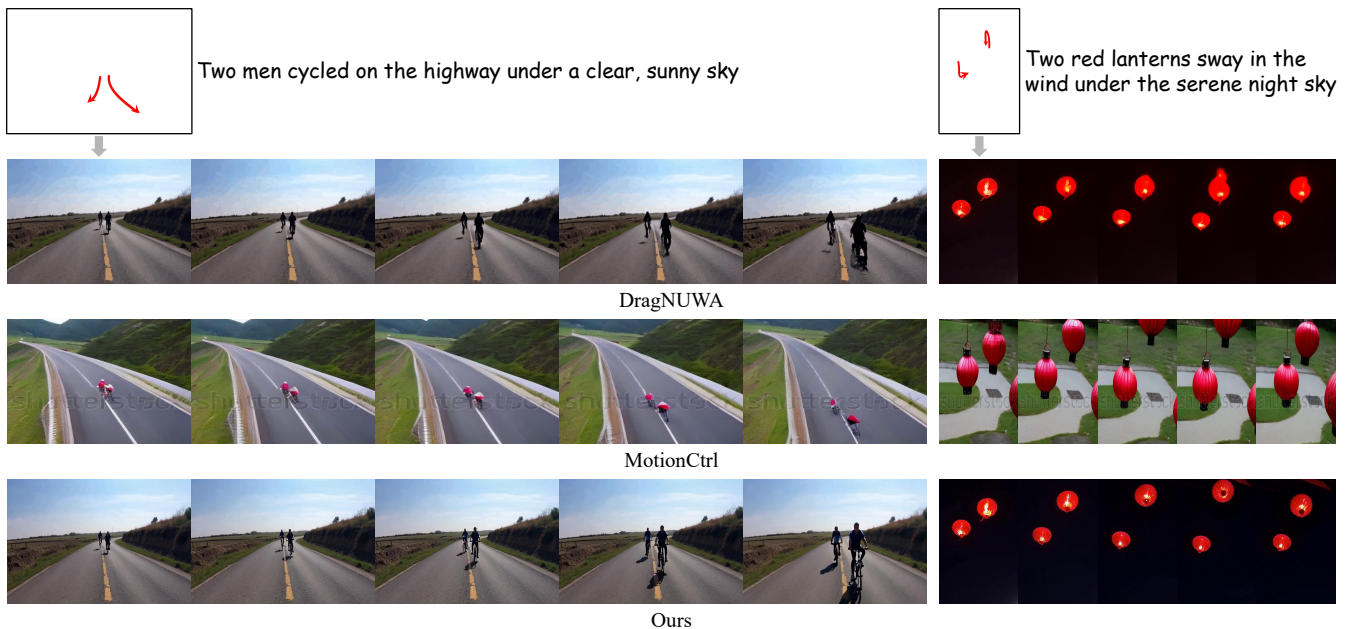


Figure 6: Qualitative Comparisons on Trajectory Control. All methods are capable of generating objects that follow the given trajectory. However, Tora not only adheres precisely to the specified trajectory but also produces smoother movement that conforms to the physics world. Please visit our supplemental materials for detailed video results.

trajectory videos with this setup yields the most favorable outcomes, underscoring the efficacy of our tailored 3D VAE approach in trajectory compression.

Block design and integrated position of MGF. We train the three variant MGF blocks as previously described, with the results presented in Table 3. Notably, the adaptive norm block achieves lower FVD and Trajectory Error compared to both cross-attention and extra channel conditioning methods, while also exhibiting the highest computational efficiency. This superiority is attributed to its capability for dynamic feature adaptation based on diverse conditions without requiring strict alignment, a limitation often encountered with cross-attention. Moreover, it ensures temporal consistency by modulating the conditional information over time, which is crucial for injecting motion cues. In contrast, channel concatenation may cause information congestion, rendering motion signals less effective. During training, we observe that initializing the normalization layer as the identity function is important for achieving optimal performance. Additionally, we evaluate the integration position of the MGF module within the Spatial DiT and Temporal DiT blocks. Our findings reveal that embedding the MGF within the Temporal DiT block notably enhances trajectory motion control, as evidenced by a substantial decrease in Trajectory Error (from 23.39 to 14.25). This approach enhances the MGF’s efficiency in interacting with temporal dynamics, thereby significantly improving the fidelity of motion synthesis.

Training Strategies. We evaluate the effectiveness of the two-stage training approach, with the results summarized in Table 4. Training exclusively with dense optical flow proves

ineffective as it fails to accurately capture the intricate details of the provided sparse trajectories. On the other hand, training solely with sparse trajectories offers limited information, making the learning process more challenging. By initially training with dense flows and subsequently fine-tuning with sparse trajectories, our model demonstrates improved adaptability to various types of trajectory data. This method not only enhances overall performance but also increases the model’s versatility in handling diverse motion patterns.

Motion-guidance	FVD	CLIPSIM	TrajError
Dense Flow	601	0.2307	39.34
Sparse Flow	556	0.2334	24.73
Hybird	513	0.2358	14.25

Table 4: Ablation of the type of training trajectories. “Hybrid” denotes the proposed two-stage training strategy.

Conclusion

This paper introduces Tora, the first trajectory-oriented Diffusion Transformer framework for video generation that integrates text, image, and trajectory conditions. Tora effectively encodes arbitrary trajectories into spacetime motion patches, which align with the scaling properties of DiT, thereby enabling more realistic simulations of physical world movements. By employing a two-stage training process, Tora achieves motion-controllable video generation across a wide range of durations, aspect ratios, and resolutions. Remarkably, it can generate high-quality videos that

adhere to specified trajectories, producing up to 204 frames at 720p resolution. This capability underscores Tora’s versatility and robustness in handling diverse motion patterns while maintaining high visual fidelity. We hope our work provides a strong baseline for future research in motion-guided Diffusion Transformer methods.

References

- Bao, F.; Xiang, C.; Yue, G.; He, G.; Zhu, H.; Zheng, K.; Zhao, M.; Liu, S.; Wang, Y.; and Zhu, J. 2024. Vidu: a Highly Consistent, Dynamic and Skilled Text-to-Video Generator with Diffusion Models. *arxiv*, abs/2405.04233.
- Bar-Tal, O.; Chefer, H.; Tov, O.; Herrmann, C.; Paiss, R.; Zada, S.; Ephrat, A.; Hur, J.; Li, Y.; Michaeli, T.; Wang, O.; Sun, D.; Dekel, T.; and Mosseri, I. 2024. Lumiere: A Space-Time Diffusion Model for Video Generation. *arxiv*, abs/2401.12945.
- Blattmann, A.; Dockhorn, T.; Kulal, S.; Mendelevitch, D.; Kilian, M.; Lorenz, D.; Levi, Y.; English, Z.; Voleti, V.; Letts, A.; Jampani, V.; and Rombach, R. 2023. Stable Video Diffusion: Scaling Latent Video Diffusion Models to Large Datasets. *arXiv preprint arXiv:2311.15127*.
- Brooks, T.; Peebles, B.; Holmes, C.; DePue, W.; Guo, Y.; Jing, L.; Schnurr, D.; Taylor, J.; Luhman, T.; Luhman, E.; Ng, C.; Wang, R.; and Ramesh, A. 2024. Video generation models as world simulators.
- Chen, H.; Xia, M.; He, Y.-Y.; Zhang, Y.; Cun, X.; Yang, S.; Xing, J.; Liu, Y.; Chen, Q.; Wang, X.; Weng, C.-L.; and Shan, Y. 2023. VideoCrafter1: Open Diffusion Models for High-Quality Video Generation. *ArXiv*, abs/2310.19512.
- Chen, T.; Siarohin, A.; Menapace, W.; Deyneka, E.; Chao, H.; Jeon, B. E.; Fang, Y.; Lee, H.; Ren, J.; Yang, M.; and Tulyakov, S. 2024. Panda-70M: Captioning 70M Videos with Multiple Cross-Modality Teachers. *arxiv*, abs/2402.19479.
- Dai, Z.; Zhang, Z.; Yao, Y.; Qiu, B.; Zhu, S.; Qin, L.; and Wang, W. 2023. Fine-Grained Open Domain Image Animation with Motion Guidance. *arxiv*, abs/2311.12886.
- Dhariwal, P.; and Nichol, A. 2021. Diffusion Models Beat GANs on Image Synthesis. *ArXiv*, abs/2105.05233.
- Envato, E. 2024. mixkit:Free assets for your next video project.
- Ho, J.; Chan, W.; Saharia, C.; Whang, J.; Gao, R.; Gritsenko, A.; Kingma, D. P.; Poole, B.; Norouzi, M.; Fleet, D. J.; et al. 2022a. Imagen video: High definition video generation with diffusion models. *arXiv preprint arXiv:2210.02303*.
- Ho, J.; Salimans, T.; Gritsenko, A.; Chan, W.; Norouzi, M.; and Fleet, D. J. 2022b. Video diffusion models.
- Jeong, H.; Park, G. Y.; and Ye, J. C. 2024. VMC: Video Motion Customization using Temporal Attention Adaption for Text-to-Video Diffusion Models. In *CVPR*.
- Khachatryan, L.; Movsisyan, A.; Tadevosyan, V.; Henschel, R.; Wang, Z.; Navasardyan, S.; and Shi, H. 2023. Text2video-zero: Text-to-image diffusion models are zero-shot video generators. *arXiv preprint arXiv:2303.13439*.
- Kingma, D. P.; and Ba, J. 2015. Adam: A Method for Stochastic Optimization. In Bengio, Y.; and LeCun, Y., eds., *3rd International Conference on Learning Representations, ICLR 2015, San Diego, CA, USA, May 7-9, 2015, Conference Track Proceedings*.
- Kingma, D. P.; and Welling, M. 2013. Auto-encoding variational bayes. *arXiv preprint arXiv:1312.6114*.
- Mou, C.; Wang, X.; Xie, L.; Wu, Y.; Zhang, J.; Qi, Z.; and Shan, Y. 2024. T2I-Adapter: Learning Adapters to Dig Out More Controllable Ability for Text-to-Image Diffusion Models. In *Thirty-Eighth AAAI Conference on Artificial Intelligence, AAAI 2024*, 4296–4304.
- Olaf Ronneberger, T. B., Philipp Fischer. 2015. U-net: Convolutional networks for biomedical image segmentation. In *Medical Image Computing and Computer-Assisted Intervention–MICCAI 2015: 18th International Conference, Munich, Germany, October 5-9, 2015, Proceedings, Part III 18*, 234–241. Springer.
- Peebles, W.; and Xie, S. 2023. Scalable diffusion models with transformers. In *Proceedings of the IEEE/CVF International Conference on Computer Vision*, 4195–4205.
- Perez, E.; Strub, F.; de Vries, H.; Dumoulin, V.; and Courville, A. C. 2018. FiLM: Visual Reasoning with a General Conditioning Layer. In *Thirty-Eighth AAAI Conference on Artificial Intelligence, AAAI 2024*, 3942–3951.
- Podell, D.; English, Z.; Lacey, K.; Blattmann, A.; Dockhorn, T.; Müller, J.; Penna, J.; and Rombach, R. 2023. SDXL: Improving Latent Diffusion Models for High-Resolution Image Synthesis. *arxiv*, abs/2307.01952.
- Ramesh, A.; Dhariwal, P.; Nichol, A.; Chu, C.; and Chen, M. 2022. Hierarchical text-conditional image generation with clip latents, 2022. URL <https://arxiv.org/abs/2204.06125>, 7.
- Singer, U.; Polyak, A.; Hayes, T.; Yin, X.; An, J.; Zhang, S.; Hu, Q.; Yang, H.; Ashual, O.; Gafni, O.; et al. 2022. Make-a-video: Text-to-video generation without text-video data. *arXiv preprint arXiv:2209.14792*.
- Unterthiner, T.; van Steenkiste, S.; Kurach, K.; Marinier, R.; Michalski, M.; and Gelly, S. 2018. Towards Accurate Generative Models of Video: A New Metric & Challenges. *arXiv:1812.01717*.
- Vaswani, A.; Shazeer, N.; Parmar, N.; Uszkoreit, J.; Jones, L.; Gomez, A. N.; Kaiser, L.; and Polosukhin, I. 2017. Attention is All you Need. In *Advances in Neural Information Processing Systems 30: Annual Conference on Neural Information Processing Systems 2017, December 4-9, 2017, Long Beach, CA, USA*, 5998–6008.
- Wan-Duo Kurt Ma, W. B. K., J. P. Lewis. 2023. TrailBlazer: Trajectory Control for Diffusion-Based Video Generation. *arXiv preprint arXiv:2401.00896*.
- Wang, X.; Yuan, H.; Zhang, S.; Chen, D.; Wang, J.; Zhang, Y.; Shen, Y.; Zhao, D.; and Zhou, J. 2023a. VideoComposer: Compositional Video Synthesis with Motion Controllability. *arXiv preprint arXiv:2306.02018*.
- Wang, X.; Zhang, S.; Yuan, H.; Qing, Z.; Gong, B.; Zhang, Y.; Shen, Y.; Gao, C.; and Sang, N. 2024a. A Recipe for Scaling up Text-to-Video Generation with Text-free Videos.

Wang, Z.; Yuan, Z.; Wang, X.; Chen, T.; Xia, M.; Luo, P.; and Shan, Y. 2023b. MotionCtrl: A Unified and Flexible Motion Controller for Video Generation. In *arXiv preprint arXiv:2312.03641*.

Wang, Z.; Yuan, Z.; Wang, X.; Chen, T.; Xia, M.; Luo, P.; and Shan, Y. 2024b. MotionCtrl: A Unified and Flexible Motion Controller for Video Generation. In *SIGGRAPH*.

Wu, C.; Huang, L.; Zhang, Q.; Li, B.; Ji, L.; Yang, F.; Sapiro, G.; and Duan, N. 2021. Godiva: Generating open-domain videos from natural descriptions. *arXiv preprint arXiv:2104.14806*.

Wu, J. Z.; Ge, Y.; Wang, X.; Lei, S. W.; Gu, Y.; Shi, Y.; Hsu, W.; Shan, Y.; Qie, X.; and Shou, M. Z. 2023. Tune-a-video: One-shot tuning of image diffusion models for text-to-video generation. In *Proceedings of the IEEE/CVF International Conference on Computer Vision*, 7623–7633.

Xu, H.; Zhang, J.; Cai, J.; Rezatofighi, H.; Yu, F.; Tao, D.; and Geiger, A. 2023. Unifying Flow, Stereo and Depth Estimation. *IEEE Trans. Pattern Anal. Mach. Intell.*, 45(11): 13941–13958.

Xu, L.; Zhao, Y.; Zhou, D.; Lin, Z.; Ng, S.; and Feng, J. 2024. PLLaVA : Parameter-free LLaVA Extension from Images to Videos for Video Dense Captioning. *arxiv*, abs/2404.16994.

Yin, S.; Wu, C.; Liang, J.; Shi, J.; Li, H.; Ming, G.; and Duan, N. 2023. Dragnuwa: Fine-grained control in video generation by integrating text, image, and trajectory. *arXiv preprint arXiv:2308.08089*.

Yu, L.; Cheng, Y.; Sohn, K.; Lezama, J.; Zhang, H.; Chang, H.; Hauptmann, A. G.; Yang, M.-H.; Hao, Y.; Essa, I.; et al. 2023a. Magvit: Masked generative video transformer.

Yu, L.; Lezama, J.; Gundavarapu, N. B.; Versari, L.; Sohn, K.; Minnen, D.; Cheng, Y.; Gupta, A.; Gu, X.; Hauptmann, A. G.; Gong, B.; Yang, M.; Essa, I.; Ross, D. A.; and Jiang, L. 2023b. Language Model Beats Diffusion - Tokenizer is Key to Visual Generation. *arXiv*, abs/2310.05737.

Zhang, S.; Wang, J.; Zhang, Y.; Zhao, K.; Yuan, H.; Qin, Z.; Wang, X.; Zhao, D.; and Zhou, J. 2023a. I2VGen-XL: High-Quality Image-to-Video Synthesis via Cascaded Diffusion Models. *arXiv preprint arXiv:2311.04145*.

Zhang, Y.; Wei, Y.; Jiang, D.; Zhang, X.; Zuo, W.; and Tian, Q. 2023b. ControlVideo: Training-free Controllable Text-to-Video Generation. *arXiv preprint arXiv:2305.13077*.

Zhao, R.; Gu, Y.; Wu, J. Z.; Zhang, D. J.; Liu, J.; Wu, W.; Keppo, J.; and Shou, M. Z. 2023. MotionDirector: Motion Customization of Text-to-Video Diffusion Models. *arxiv*, abs/2310.08465.

Zhao, W.; Liu, S.; Guo, H.; Wang, W.; and Liu, Y. 2022. ParticleSfM: Exploiting Dense Point Trajectories for Localizing Moving Cameras in the Wild. In *Computer Vision - ECCV 2022 - 17th European Conference, Tel Aviv, Israel, October 23-27, 2022, Proceedings, Part XXXII*, volume 13692, 523–542.

Zheng, Z.; Peng, X.; Yang, T.; Shen, C.; Li, S.; Liu, H.; Zhou, Y.; Li, T.; and You, Y. 2024. Open-Sora: Democratizing Efficient Video Production for All.